Transactions, **SMiRT-25**
Charlotte, NC, USA, August 4-9, 2019
Division I: Mechanics of Materials

EFFECTS OF ALKALI-SILICA REACTION ON MECHANICAL PROPERTIES AND STRUCTURAL CAPACITIES OF REINFORCED CONCRETE STRUCTURES

Long Phan[1], Fahim Sadek[2], Travis Thonstad[3], H.S. Lew[4], Sorin Marcu[5], Jacob Philip[6]

[1] Leader, Structures Group, NIST, MD, USA (long.phan@nist.gov)
[2] Research Structural Engineer, NIST, MD, USA (fahim.sadek@nist.gov)
[3] Research Structural Engineer, NIST, MD, USA (travis.thonstad@nist.gov)
[4] Senior Research Structural Engineer, NIST, MD, USA (hai.lew@nist.gov)
[5] Engineer Technician, NIST, MD, USA (sorin.marcu@nist.gov)
[6] Senior Geotechnical Engineer, NRC, MD, USA, (Jacob.philip@nrc.gov)

ABSTRACT

This paper describes an ongoing, comprehensive research program being conducted at the National Institute of Standards and Technology (NIST) under the sponsorship of the U.S. Nuclear Regulatory Commission (NRC). The study aims to develop technical basis for evaluating effects of Alkali-Silica Reaction (ASR), which occurs when the high pH concrete pore solution reacts with certain aggregate mineral phases to form expansive ASR gel and create internal expansive forces that cause cracking in concrete, on engineering properties and structural capacities of reinforced concrete structures. Description of this study focusing on experimental evaluation of: (1) the influence of different degrees of steel confinement and ASR expansions (0.1%; 0.3%; 0.5% ultimate expansion) on concrete's mechanical properties; (2) effects of ASR on the bonding between concrete and reinforcements (development and lap splice lengths) and on overall flexural capacities of reinforced concrete beams; and (3) effects of ASR on seismic performance of typical reinforced concrete walls with and without steel confinement in the wall boundary element, will be provided.

INTRODUCTION

Alkali-silica reaction (ASR) has long been recognized as a major cause of concrete internal cracking and deterioration (Stanton 1940; Swenson 1957). This concrete deterioration mechanism begins with reaction between the alkali hydroxides in the cement paste and certain amorphous or micro-crystalline siliceous phases in the aggregates, which produces an alkali-silica gel that forms initially in the partially saturated pore space of the hardened cement paste. The alkali-silica gel is hygroscopic and will continue to absorb moisture in the concrete matrix and expand. This expansion is not reversible and will continue over time as long as moisture is present. The continued expansion of alkali-silica gel creates increasing internal pressure that ultimately leads to internal cracking and degradation of the mechanical properties of concrete (Hansen 1944, Taylor 1990).

Generally, the rate of ASR expansion is relatively slow and is a function of the reactivity of the mineral phases, the alkalinity of the pore solution, and the availability of moisture. Thus, the onset of ASR-induced cracking can take years or decades after construction to occur. However, once occurred, this deterioration at the material level may affect the bonding characteristics between the concrete and the reinforcement and the overall capacity and service life of reinforced concrete structural member or system.

At present, the industry solution is to identify the reactive aggregates and avoid using them through sourcing of materials for construction. This would help with avoiding ASR problem in new construction but does not address the problem in existing structures. Given the current lack of knowledge on ASR effects and standards and codes provisions to account for the effects of ASR on structural capacities, the questions of how to (1) predict the progression of ASR-induced deterioration once occurred and (2) assess the residual material properties and in-situ structural capacity of the affected structures, especially if they are safety-related facilities that are required to maintain a certain safety margin over an extended period of service life, become extremely relevant for certain critical components of the nation's infrastructure (e.g., dams, bridges, and nuclear power plants). Accurate predictions of the progression of ASR and future, residual structural capacities can provide critical support for decision on whether the affected structures can continue safe operation or if it is time for cessation of operations given the increased risk to public safety.

This paper describes work that is part of a comprehensive research program being conducted by the Engineering Laboratory of the National Institute of Standards and Technology (NIST) to study the effects of ASR on the structural performance of nuclear power plant concrete structures. The work is funded by the U.S. Nuclear Regulatory Commission (NRC) under Inter-Agency Agreement NRC-HQ-60-14-I-0004. The objective of this research program is to develop the technical basis for generic regulatory guidance for evaluation of ASR-affected nuclear power plant (NPP) concrete structures throughout its service life. Specifically, the program will develop measurements for evaluation of (1) effects of ASR on structural performance and capability to perform intended function under design basis static and dynamic loads, and (2) characteristics of an asset management program to adequately monitor and manage aging effects of ASR degradation such that intended functions are maintained through the period of extended operation of renewed licenses. The intended outcome is a methodology for determining for an existing ASR-affected structure (1) the in-situ structural capacity to resist design-basis static and dynamic loads and (2) future structural capacity.

NIST EXPERIMENTAL PROGRAM

The NIST experimental program is comprised of two parts. Part 1 focuses on effects of ASR on concrete material properties and performance of reinforced concrete structures subjected to static and pseudo-dynamic loadings. Part 2 examines degradation mechanisms of concrete at micro-structural level. This paper describes Part 1 of the NIST research program focusing on concrete mixture design and curing to achieve certain level of ASR expansion, and the test plan for assessing the effects of ASR on (1) concrete mechanical properties, (2) bonding characteristic and anchorage of steel reinforcement and flexural capacity of reinforced concrete beams, and (3) seismic performance of reinforced concrete walls.

Concrete Mixture Proportioning and Curing

To facilitate examination of the effects of different degrees of ASR expansion on structural capacities of reinforced concrete structural members, four concrete mixtures, namely ASR1 to ASR4, were developed. The first three mixtures, ASR1, ASR2, and ASR3, were designed to have ASR with specific ultimate expansions ε_{ASR} of 0.15%; 0.3%; and 0.5%, respectively. These ultimate expansion levels, from low (ε_{ASR} = 0.15%) to high (ε_{ASR} = 0.5%), were achieved using Type I/II cement with minimum alkali equivalent (Na_2O) content of ≥ 0.87%, alkali reactive coarse aggregate (Placitas, sourced from Albuquerque, New Mexico), and different combinations of reactive (Jobe, sourced from El Paso, TX) and non-reactive (Chaney, sourced from Hagerstown, MD) fine aggregates that meet the grading specification of ASTM C33. The fourth mixture (ASR4) was designed to be non-reactive, utilizing Type I/II cement with low alkali equivalent (Na_2O) content (<0.87%) and non-alkali reactive aggregates, for use in reference specimens for comparison purpose. All coarse aggregates have a maximum size of ¾ inch (20 mm). All four mixtures utilized high range water reducer (BASF MasterGlenium 7710 for the three reactive concrete mixtures and Sika 2100 for the non-reactive control mixture) that complies with ASTM C494 to aid with workability. Table 1 shows the mixture proportioning for the concretes used in the NIST experimental program.

Table 1: Mixture Proportioning for Concretes in the NIST Experimental Program

	Cement Content			**Coarse Aggregate**			**Fine Aggregate**			**Alkalis ***	**Water**
Mixture	**Type**	**lb/yd³ (kg/m³)**	**vol. fraction**	**Type**	**lb/yd³ (kg/m³)**	**vol. fraction**	**Type**	**lb/yd³ (kg/m³)**	**vol. fraction**	**lb/yd³ (kg/m³)**	**Gal (lb/yd³)**
ASR 1	I/II, high alkali (≥0.87 % Na_2O)	588 (350)	0.111	Placitas	1767 (1050)	0.420	Chaney	1199 (713)	0.274	4.90	35 (294)
ASR 2	"	588 (350)	0.111	"	1767 (1050)	0.420	Jobe Chaney	711 (423) 480 (285)	0.274	4.90	35 (294)
ASR 3	"	588 (350)	0.111	"	1767 (1050)	0.420	Jobe	1185 (705)	0.274	4.90	35 (294)
ASR 4	I/II, low alkali (≤0.87 % Na_2O)	578 (343)	0.115	#57	1805 (1071)	0.399	Washed #33 Sand	1385 (822)	0.295	<2.0	35 (294)

* Total alkali content, including cement alkali + NaOH addition.

Typical curing conditions to accelerate ASR in laboratory conditions involve wetting the top surface prior to form removal and covering the test specimens with wet burlap and plastic sheets after form removal for the first 90 days after casting, at normal ambient temperature and relative humidity, to prevent excessive moisture loss on the specimen's surface layer and minimize potential for drying shrinkage cracks during the hydration process. At 90 days of age, the plastic and burlap covers were removed and the curing temperature and relative humidity in the curing chamber were increased to 75°F (24 ºC) and 75 %. At 180 days of age, the relative humidity was increased again to the range of 95 % to 100 %. The 75°F (24 ºC) and 95 % - 100 % relative humidity curing conditions were then maintained until test time.

Assessing In-Situ Mechanical Properties of ASR-Affected Concrete

This task aims to assess the relationship between ASR-induced expansion and: (1) concrete mechanical properties; (2) surface cracking and expansion, and (3) the influence of hoop reinforcement (i.e., stirrups) on the expansion through measurements conducted on four large block specimens, 3.5 ft × 6 ft × 16 ft (1.07 m × 1.83 m × 4.88 m). Three of the block specimens were made with the ASR1, ASR2, and ASR3 concretes shown in Table 1, and the fourth specimen was made with non-reactive ASR4 concrete and served as the control specimen.

For reinforcement, each block specimen was divided into three regions (Regions 1 to 3, see Figure 1), each region was isolated by a 2-inch (51-mm) thick polystyrene divider to minimize the possible interaction of expansion with the adjoining region and reinforced longitudinally with a combination of #8 and #10 headed bars and transversely with #8 and #10 stirrups and cross ties. The variation in the bar sizes used in each region and inclusion of cross ties in Region 3 were designed to produce different degrees of concrete confinement in the three regions of each block specimen (see Figure 2). Region 2 of each block specimen was not transversely reinforced (no stirrups, reinforcement ratio in the transverse and vertical, or x and y, directions $\rho_x = \rho_y = 0\%$) and will provide measurements of concrete material properties and cracking characteristics corresponding with the unconfined expansion condition. Region 1 measurements will correspond with intermediate level of expansion confinement ($\rho_x = 0.2\%$), and Region 3 measurements will correspond with a higher level of expansion confinement ($\rho_x = 0.6\%$).

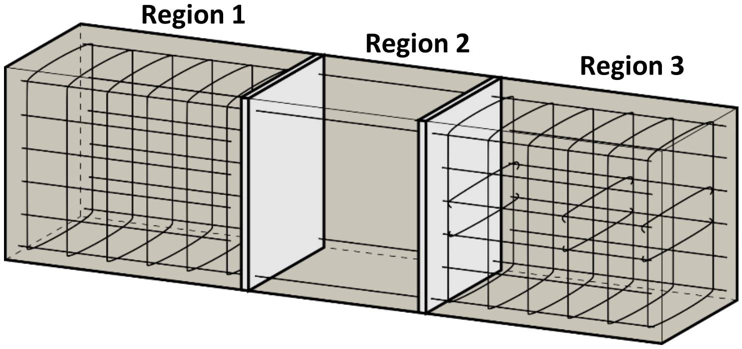

Figure 1. Regions and Reinforcement Scheme of Block Specimen.

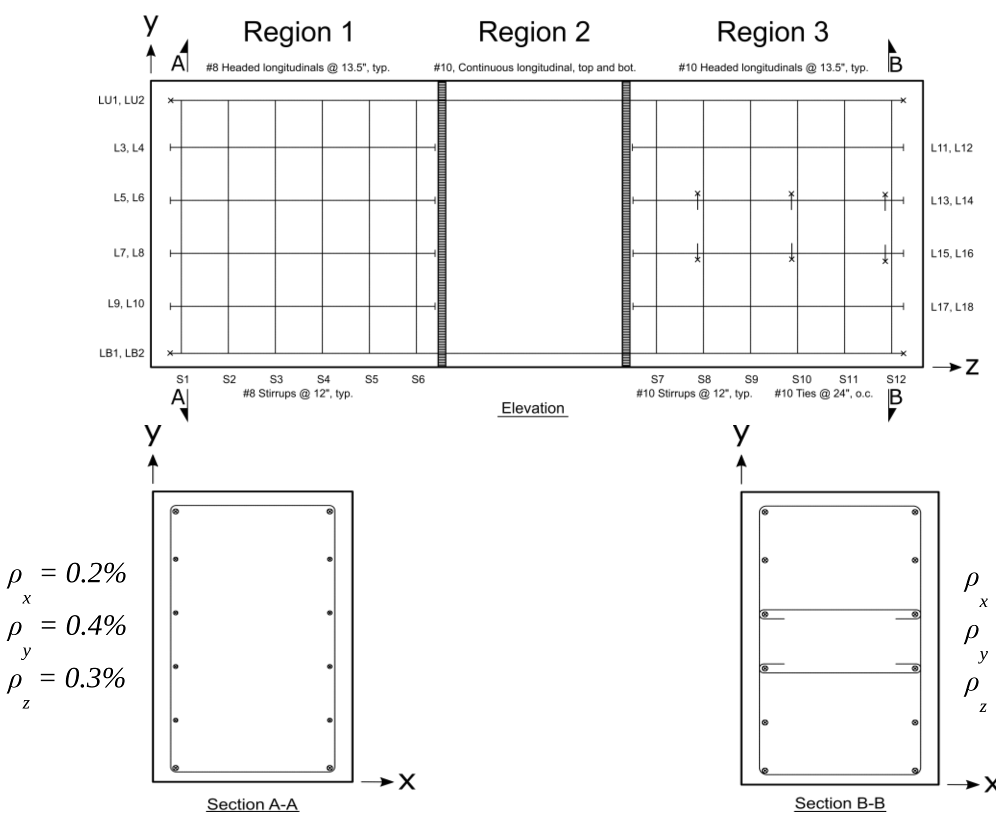

Figure 2. Reinforcement Details of Block Specimen.

All four block specimens were heavily instrumented, each with approximately 164 strain gages attached to the reinforcements, strain transducers to measure tri-directional concrete strain, as well thermo-couples and wireless relative humidity sensors. Figure 3 shows the typical strain gage instrumentation scheme. ASR-induced expansion of concrete, evidenced by increasing strain over time in the reinforcement, are measured and recorded continuously. Figure 4 shows a sample time-history of ASR-induced strain development in the reinforcement in Region 1 of ASR3 block specimen. The time-history provides a correlation between the rates of concrete expansion and the curing conditions and indicates yielding of longitudinal reinforcements shortly before 480 days of curing for this specimen. Correlation of degree of ASR expansion with changes in concrete mechanical properties as a function of time and different levels of confinement is performed through mechanical properties testing of concrete cylinders and cores extracted from different regions of the block specimens. Surface expansion is monitored by measuring changes in vertical and horizontal distances between targets that form square grid (10 ¾ × 10 ¾) on the side of the block specimens using laser tracking device and high-precision calliper.

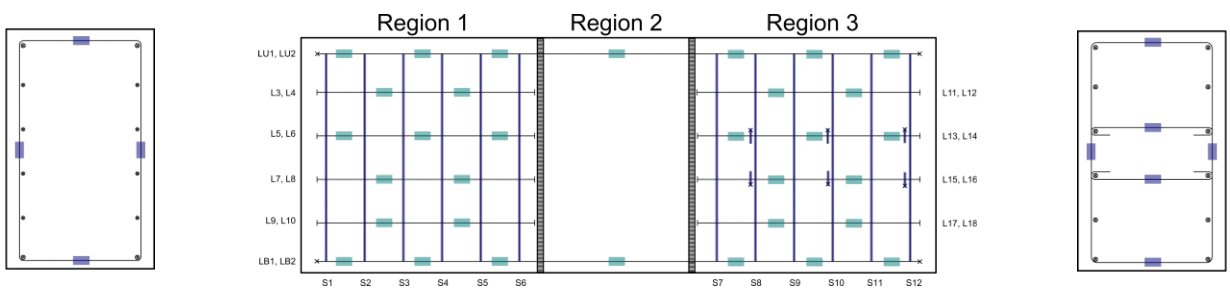

Figure 3. Locations of Strain Gages on the Reinforcements of the Block Specimen.

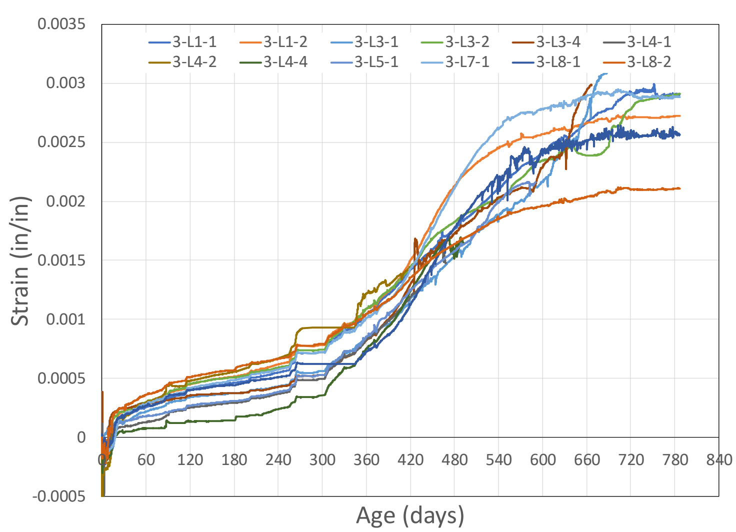

Figure 4. Time-Histories of Strain Development in Region 1 of ASR3 Block Specimen.

Concrete cylinders and cores extracted from different regions of the block specimens are tested periodically for time-histories of concrete compressive strength, splitting tensile strength, and elastic modulus. Data are being processed and compared for evaluation of effects of ASR on concrete mechanical properties. Comparison will also be made with ACI empirical equations to assess applicability of these equations to ASR-affected concrete.

Assessing Bond and Anchorage of Steel Reinforcement

This task aims to examine how ASR influences (1) the bonding characteristic between concrete and steel reinforcement, both for continuous, axially loaded, reinforcing bars and for lap splices in flexural members and (2) the possible loss of rebar anchorage and overall reduction of member's flexural capacities. To facilitate this examination, a series of 19 beam specimens, consisting of 16 reactive beams made of ASR3 concrete and 3 reference, non-reactive beams (also made of ASR3 concrete but with addition of Lithium Nitrate to neutralize the ASR), were constructed and tested under four-point bending. The test series was designed to facilitate examination of the effects of the following three main variables, as well as their interactions, on flexural capacities of reinforced concrete beams: degree of ASR expansion ($\varepsilon_{ASR}(t)$); degree of concrete confinement (K_{tr}/d_b); and ratio of lap splice and development length (l_s/l_d). The test matrix for this test series is shown in Table 2. Beam dimensions and test configuration are shown in Figure 5. Values of $\varepsilon_{ASR}(t)$ shown in Table 2 indicate the nominal expansion level, measured as maximum strain in the reinforcement, relative to the target expansion level $\varepsilon_{ASR}(t)$ = 0.3% for ASR3 concrete when the beam is to be tested (e.g., beam specimen 1, with $\varepsilon_{ASR}(t)$ = 25%, is to be tested when the ASR-induced expansion has resulted in a nominal strain in the reinforcement in the amount of 25% × 0.3% = 0.00075 in/in).

Table 2. Beam Test Matrix

Specimen	$\varepsilon_{ASR}(t)$ **(% of ASR3 Target Expansion at Test Time)**	K_{tr} / d_b	l_s / l_d
1	25%	0.5	0.7
2	25%	0.5	1.3
3	25%	1.5	0.7
4	25%	1.5	1.3
5	75%	0.5	0.7
6	75%	0.5	1.3
7	75%	1.5	0.7
8	75%	1.5	1.3
9	50%	1.0	1.0
10	50%	1.0	Continuous Bar
11	Non-Reactive	1.0	1.0
19	100%	1.0	1.0
13	50%	0.0	1.0
14	50%	1.8	1.0
15	50%	1.0	0.5
16	50%	1.0	1.5
17	Non-Reactive	1.0	1.0
18	Non-Reactive	1.0	Continuous Bar
19	100%	1.0	1.0

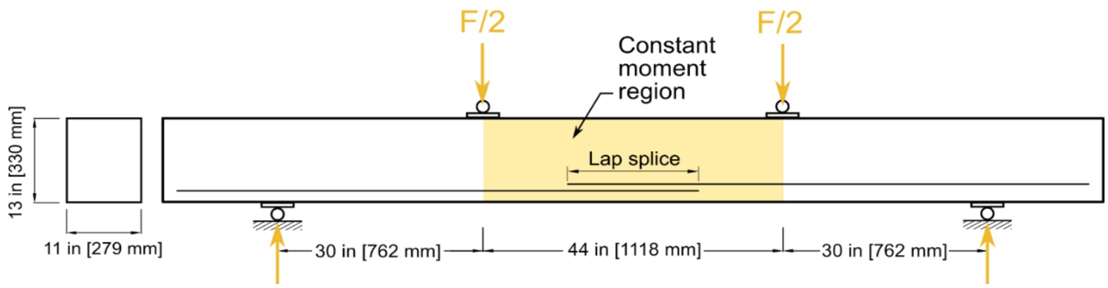

Figure 5. Beam Dimensions and Test Configuration

To date, 16 of 19 beams have been tested. Data analysis is being conducted to examine the effects of the mentioned variables on the bonding characteristic, anchorage strength, and overall flexural beam capacities. Results of the analysis and findings will be presented in a more detailed report to the project sponsor at a later date. Preliminary test results, in the form of maximum vertical load vs. maximum mid-span deflection, are shown in Figure 6. This plot shows the varied modes of failure observed in the 16 tested beams, which ranged from bond failure prior to yielding of the tension reinforcement, yielding of tension reinforcement followed by bond failure, and yielding of tension reinforcement followed by compression failure of concrete in the compression zone.

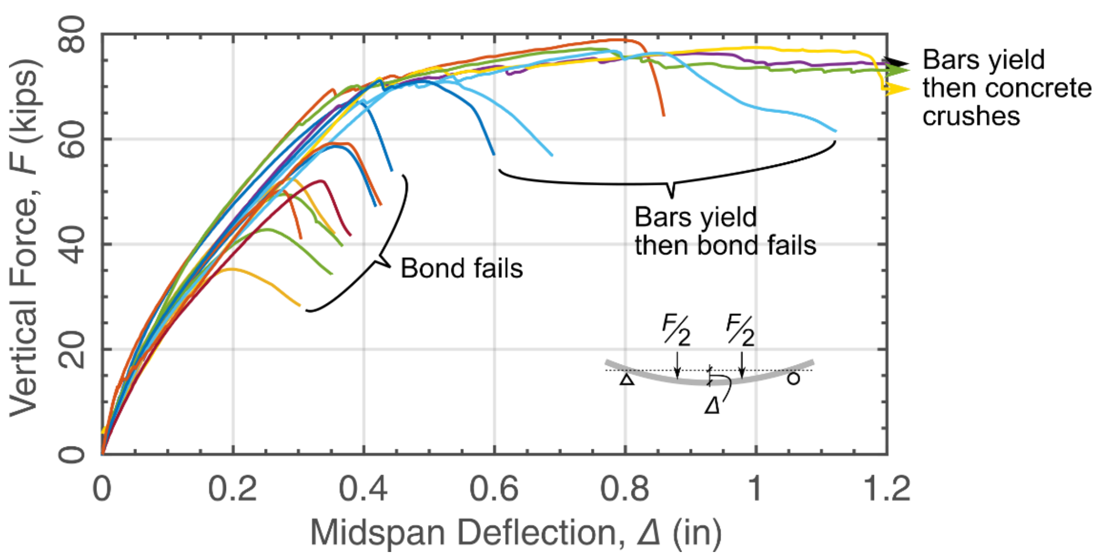

Figure 6. Maximum Load vs. Mid-Span Deflection of Beams

1 kip = 4.45 kN
1 inch = 25.4 mm

Assessing Seismic Performance of ASR-Affected Structural Walls

This task aims to assess the effects of ASR on seismic capacity of typical reinforced concrete walls. Seismic capacities – in terms of lateral stiffness, ultimate strength, ductility, and energy dissipation – of four reinforced concrete wall specimens will be measured through pseudo dynamic cyclic lateral load tests. Three of the wall specimens are made of reactive ASR3 concrete and the fourth non-reactive concrete made of ASR3 concrete modified with Lithium Nitrate (reference specimen). Experimental variables to be studied include (1) degree of ASR expansion $\varepsilon_{ASR}(t)$ and (2) degree concrete confinement, represented by the transverse reinforcement ratio, in the wall's boundary element (ρ_s). Figure 7 shows the dimensions and typical reinforcement details on a cross section of a wall specimen. Table 3 shows the test matrix for this series of wall seismic lateral load test. For testing, the wall specimens are subjected to constant axial compression load to simulate service load while simultaneously subjected to cyclic lateral displacement with increasing magnitude, as shown in Figure 8. At present, the wall specimens have been constructed and are being cured to accelerate ASR expansion for testing.

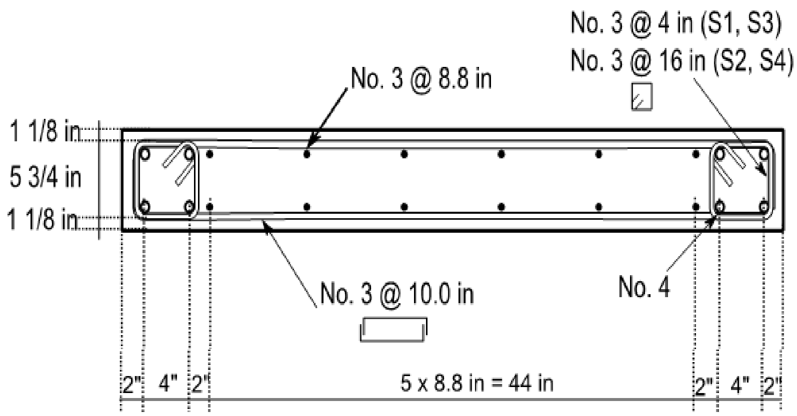

Figure 7. Cross-Sectional Dimensions and Reinforcement Details of Wall Specimen

1 inch = 25.4 mm

Table 3. Wall Lateral Load Test Matrix

Wall Specimen	**$\varepsilon_{ASR}(t)$ (% of ASR3 Ultimate Expansion at Test Time)**	**ρ_s**
1	50%	0%
2	100%	2%
3	100%	0%
4	Non-Reactive	2%

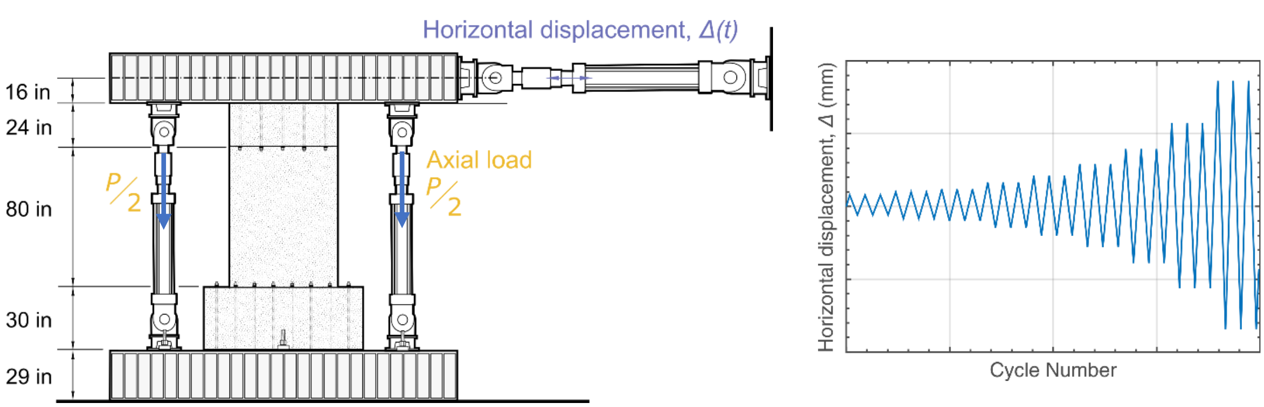

Figure 8. Wall Test Set-up and Loading Scheme

SUMMARY

An experimental plan to measure and quantify the effects of ASR on concrete material properties and structural capacities of reinforced concrete beam and walls, being conducted at NIST under the sponsorship of the NRC, is described. Measurements obtained from this study will be used to develop a methodology for determining the in-situ and future structural capacity of ASR-affected structure and will form the technical basis underpinning possible generic regulatory guidance for evaluation of ASR-affected nuclear power plant (NPP) concrete structures throughout its service life. Discussions of test results and findings will be provided in detail in subsequent joint NIST/NRC publications.

DISCLAIMER

Certain commercial equipment, instruments, or materials are identified in this paper to foster understanding. Such identification does not imply recommendation or endorsement by the National Institute of Standards and Technology, nor does it imply that the materials or equipment identified are necessarily the best available for the purpose.

REFERENCES

ASTM C33. 2018. *Standard Specification for Concrete Aggregates.* ASTM International. West Conshocken, PA.

ASTM C494. 2017. *Standard Specification for Chemical Admixtures for Concrete.* ASTM International. West Conshocken, PA

Stanton, T.E. 1940. *"Expansion of concrete through reaction between cement and aggregate."* Proceedings of the American Society of Civil Engineers, 66(10): 1781-1811.

Swenson, E.G. 1957a. *"A reactive aggregate undetected by ASTM tests."* Proceedings of American Society for Testing and Materials, 57, 48-51.

Swenson, E.G. 1957b. "Cement aggregate reaction in concrete of a Canadian bridge." ASTM Proceedings, 57 1043–1056.